Up Goer 4

Final Report

May 6, 2015
Group 5 – Balsa Bombers
Michael Martel, Erik Nelson, Cecilia Ruiz, John Sontag

Table of Contents

List of Figures

List of Tables

Conceptual Design

Design Drivers

We propose to design an aircraft that will serve as an air taxi for the Crazy Air Taxi Planes, LLC (CATplanes). They are an air taxi service focused on getting their patrons to their destinations quickly while providing a thrilling experience. The goal is to create a prototype remote controlled aircraft to compete for a contract.

The design goal of this vehicle is to offer a fast commute while still keeping in mind the safety of our passengers. The airplane will fly a flight path that includes a 360 degree turn and a length of distance of roughly 1000 feet. As a result, the goal is to create a fast, maneuverable and safe aircraft.

The intent of our design is to focus on the maneuverability of our vehicle in order to provide the quickest and safest flight experience. Our power plant will be supplied by CATplanes and therefore will be the same as the rest our competition. As a result, our main design driver is to optimize our turn rate for the purpose of creating a highly maneuverable plane.

Wing Design

With turn rate as our primary design driver, wing loading was selected to give the fastest turn rate. For a more maneuverable plane, it is best to have a low wing loading. As a result we chose to set our wing loading as close to 1.5 lb. /ft.^{2} as possible.

When analyzing the equations for instantaneous and sustained turn rates, shown below, another important design characteristic we chose to focus on was that of aspect ratio.

$$\dot{\psi}_{instantaneous} = \frac{g\sqrt{n^2 - 1}}{V}$$

$$\dot{\psi}_{max-s} = \frac{g\sqrt{\frac{q\pi Ae}{W/S}\left[\left(\frac{T}{W}\right)_{max} - \frac{qC_{D_0}}{W/S}\right] - 1}}{V}$$

As shown in the sustained turn rate equation, a higher aspect ratio combine with a low wing loading will give us optimum rates. As a result, we chose to set our aspect ratio to 10. By choosing a wing loading of 1.5 lb./ft^2 and an estimated weight of 6.5 lbs. (shown in Table 1), the area of our wing was calculated as 4 ft^2. These design decisions combined with our airfoil data explained further below, allowed us to use the above equations to estimate an instantaneous turn rate of 84 degrees per second and a sustained turn rate of 68 degrees per second.

Table 1. Weight Estimate

Component	**Weight**
Payload	2.05 lbs.
Propeller	0.058 lbs.
Engine/Mount	0.714 lbs.
Battery	0.766 lbs.
Other (i.e. servos, landing gear)	1.293 lbs.
Structure Weight	1.619 lbs.
Total	**6.5 lbs.**

The relations used to design the main wing were incorporated into the spreadsheet shown in Figure A-1 of Appendix A. The important airfoil data that were needed for the proposed jet wing design calculations were $C_{l_{max}}$, $C_{l_{\alpha}}$, the location of the aerodynamic center, the zero-lift angle of attack, the base drag coefficient, the leading edge radius, and the extent of the drag bucket. The other inputs needed that were determined at this stage were the leading-edge sweep angle, the maximum thickness-to-chord ratio, and the taper ratio. In addition to these newly determined parameters, the data that have already been specified or determined in the design that are needed as inputs are the wing area, the wing aspect ratio, the cruise Mach number, the cruise altitude, the weight at the start and end of cruise, and the dynamic pressure at the start and end of cruise.

The cruise Mach number was calculated using the known propulsion parameters. This resulted in a Mach number of 0.06. A high aspect ratio of 10 was chosen for the purposes of maneuverability as previously described. Wing loading at each phase of flight was determined as explained in the previous section. The wing loading analysis gave W/S = 1.6 lb. /ft^2. This value along with the dynamic pressure at cruise altitude were used as inputs in the design parameters for the spreadsheet.

Because the plane will be flying at low Reynolds number, an Eppler airfoil was chosen. The specific section chosen was an Eppler E193. Its characteristics, shown in Table 2, were used as input parameters for the spreadsheet.

Table 2. Main wing airfoil characteristics.

Airfoil Data		
Name	*Eppler E193*	
Cl_{max}	1.3	
Cl_{α}	0.11	1/deg
a.c.	0.25	c
α_{0L}	-3	deg
C_{d0}	0.01	
r_{le}	0.015	c
Cl_{minD}	0 - 5	
(t/c)max	0.10	c

A taper ratio of 0.40 was chosen and the decision was made to not have a leading-edge sweep angle. We chose to add a taper to our wing because it gives the most ideal form of lift distribution since the wing planform is closer to the ideal ellipse shape. As for the leading-edge sweep, the decision to not have the sweep was made because we did not believe that the aerodynamic benefits would be as significant on a small scale aircraft. The thickness to chord ratio was set as 0.10 to get a higher $C_{l_{max}}$ according to our airfoil's characteristics. The results of our chosen parameters gave a wing span of 6.3 ft. with a mean aerodynamic chord of 0.7 ft.

For this design, the drag coefficient for the wing at cruise was determined to be C_D = 0.007. In determining the base drag coefficient, C_{D_0}, the form factor was calculated as 1.30. The value for C_{D_0} in this case is 0.006, giving an overall drag force at cruise Mach number and altitude of 0.136 pounds. The total wing *L/D* for this design is 13.5.

Vertical and Tail Design

For the vertical stabilizer, a size coefficient, C_{VT}, of 0.07 was chosen. This number was based on the coefficient from Table 6.1 (Corke, 123) for a fighter plane since our goal is to make a maneuverable aircraft. The length, L_{VT}, was chosen as 2.3 ft. A side view drawing of the aircraft showing the fuselage, main wing, and vertical tail is shown in Figure 1. A taper ratio of $\lambda = 0.40$ was chosen. An aspect ratio of $A_{VT} = 1.00$ was determined by the range specified in Table 6.5 (Corke, 127).

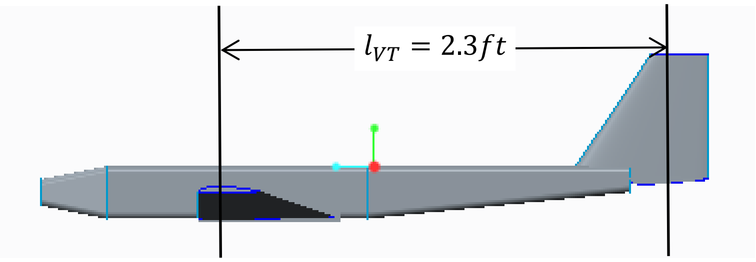

Figure 1. Side-view drawing showing locations of main wing and vertical tail on fuselage.

Once again, Eppler airfoils were chosen for the horizontal tail due to the low Reynolds number our aircraft will be flying at. For the horizontal and vertical tails the section chosen was an Eppler E472. This is a symmetric airfoil in the same family as the airfoil used for the main wing. With these decisions, the calculations resulted in the following vertical tail design described in the following table.

Table 3. Vertical Tail Design.

$\boldsymbol{S_{VT}}$	0.7840 ft.^{2}
$\boldsymbol{b}$	0.8 ft.
$\boldsymbol{c_r}$	0.9 ft.
$\boldsymbol{c_t}$	0.36 ft.
$\boldsymbol{dC_L/d\alpha}$	0.024 per degree
$\boldsymbol{C_{D_o}}$	0.004674

For the horizontal stabilizer, size coefficient, $C_{HT} = 0.40$, was chosen. This was based on the coefficient from Table 6.1 (Corke, 123) for a fighter plane. The length, L_{HT}, was chosen as 2.3 ft., for a conventional tail design. A top view drawing of the aircraft showing the fuselage, main wing, and horizontal tail, is shown in Figure 2. A taper ratio of $\lambda = 1.00$ was chosen to make the stabilizer a flat plate. An aspect ratio of $A_{HT} = 3.0$ was determined by the range specified in Table 6.5 (Corke, 127).

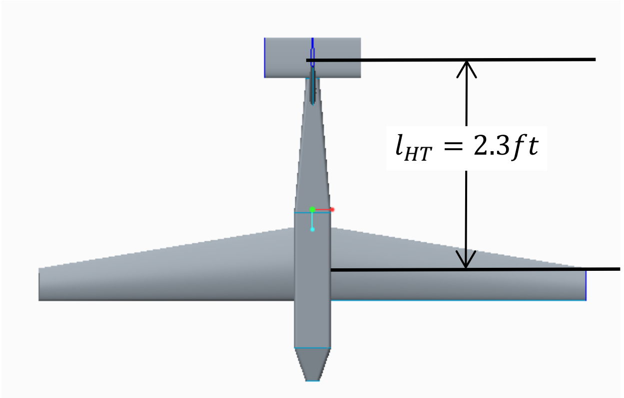

Figure 2. Top-view drawing showing locations of main wing and horizontal tail on fuselage.

Though the calculations from the spreadsheet, shown in Figure A-2, gave a good starting point for our horizontal tail size, we decided to increase the stabilizer based on the scaling recommendations from the pilots. The area was increased to 0.6 ft^2. The following table shows the final horizontal tail design size.

Table 4. Horizontal Tail Design.

S_{HT}	0.6 ft.^{2}
b	1.2 ft.
c_r	0.5 ft.
c_t	0.5 ft.
$dC_L/d\alpha$	0.059 per degree
C_{D_0}	0.007076

Preliminary estimates gave a drag on the vertical stabilizer as 0.019 lbs. and on the horizontal stabilizer as 0.018 lbs. Together the total drag on the tail design adds up to 0.037 lbs.

Control Surfaces Design

Per the recommendations shown in the following figures from the pilots' scaling recommendations, we've decided on the following control surface percentages.

Table 5. Control surface decisions.

Control Surface	Percentage
Elevator	30% of the horizontal tail
Rudder	38% of the vertical tail

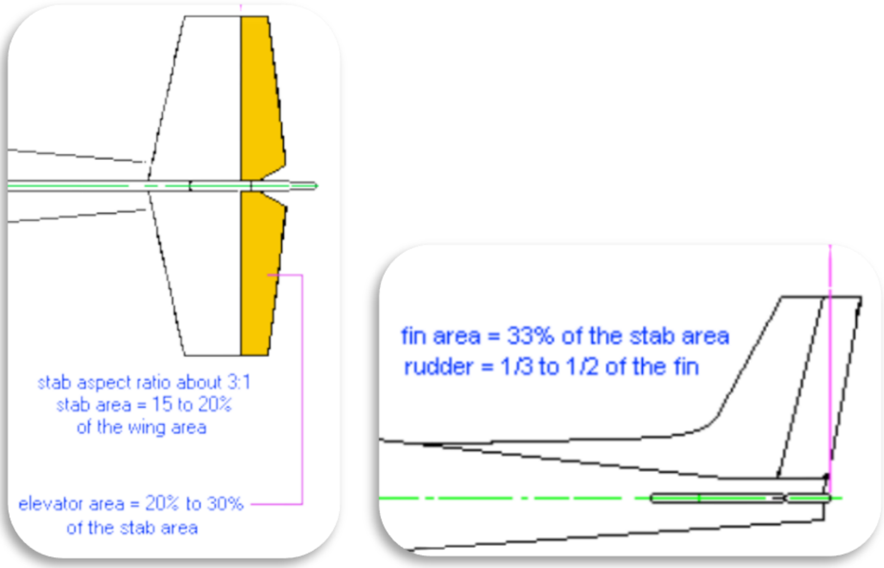

Figure 3. Pilot scaling recommendations. (Photos taken from Trainer Scaling PDF provided on the Aerospace Design website)

Payload Configuration

The passenger configuration moving aft is one Lou, one Bubba, one Ted, one Dolly, two Snoopys, and one Ted. The first three passengers will be placed before the wing box. Dolly and the two

Snoopys will lie on top of the wing box where they can easily be moved to properly place the center of gravity. Ted will be placed as far aft as possible in the cargo bay right before the tail section of the fuselage. The total weight of the passenger payload is 2.05 lbs. and will span the length of the cargo bay. The cargo bay's height and width are informed by the largest passengers with Ted, the tallest, measuring 3.75 in. high and Dolly, the widest, measuring 5 in. wide.

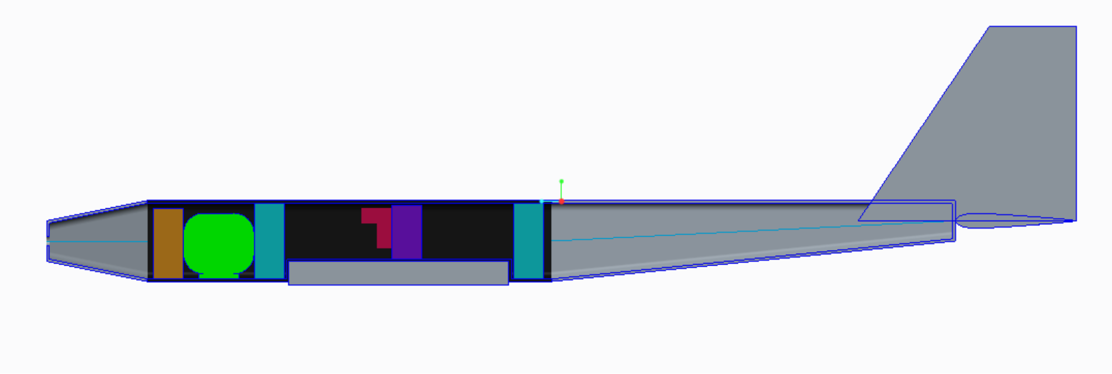

Figure 4. Side view of passenger configuration.

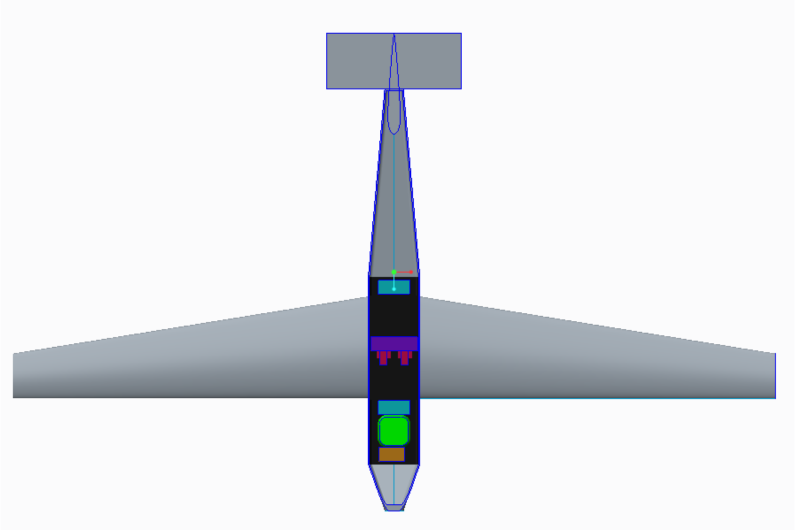

Figure 5. Top view of passenger configuration.

Fuselage Design

The proposed fuselage design is divided into three sections: the nosecone, the cargo bay, and the tail support section. The nosecone's sole purpose is to house the propeller motor. The tail support section will house the battery as well as provide a moment arm for the tail control surfaces. The cargo bay houses the passenger payload and the wing box as well as provides a support structure for the loads experienced by the wing.

The current geometry for the fuselage is as follows. A 2 x 2 in. flat panel tapers over 5 inches into a 4 x 5.5 in. section to form the nosecone. This 4 x 5.5 in. section extends uniformly over the 20 in. to form the cargo bay. At the end of the cargo bay this section sweeps over another 20 in. into a 1 x 1 in. flat panel. This tail section sweeps from the base upward meaning the top surface of the fuselage is flat over the cargo bay and tail section. This geometry yields a total fuselage length of 45 in. (3.75 feet). The proposed design incorporated a bottom-mounted wing with a dihedral of 3°. The wing box is placed 2 in. from the aft end of the cargo bay and extends forward 11 in., the length of the wing root chord, and 1 in. deep into the cargo bay. Figure 6 shows the assembled fuselage sections.

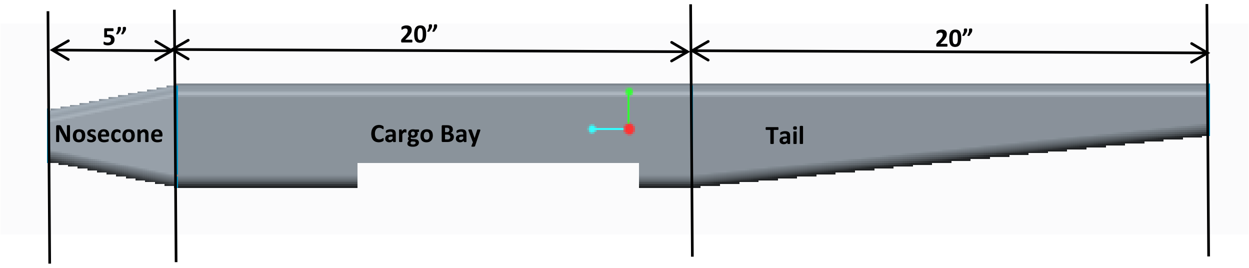

Figure 6. Side view of assembled fuselage sections.

The length of the cargo bay allows for some variation in the placement of the payload and electronics. This allows for subtle alteration of the center of mass placement post-construction to ensure flight and stability performance meets the requirements of the mission and the expectations of the pilot. In order to access the passengers and electronics in the cargo bay, we’ve designed the cargo bay to have a top cover that can be removed and attached via magnets.

Stability Prediction

After creating a detailed model of our design, we were able to properly calculate the center of gravity to make sure that our design was stable. The equations used to calculate the stability coefficients were integrated into the spreadsheets shown in Figures A-3 and A-4 in Appendix A.

Calculations for stability were done for the empty design as well as the fully loaded design. In both cases, the wing center of lift is at 14.1” from the nose.

In the case of our empty aircraft, the center of gravity is at 13.5”, giving a static margin of 0.0714. This static margin revealed that our plane is statically stable since it is greater than zero. The analysis of the longitudinal stability coefficient showed that the contribution of the wing was stabilizing. The total longitudinal stability coefficient was a stable value of $C_{M,alpha}$ = -1.59. This is actually more stable than we would like the plane but it is still within the stable range.

The analysis of the directional stability showed that our plane is stable. Our calculations resulted in a stable coefficient of C_{n_β} = 0.0824. The lateral stability coefficient was estimated as the negative of the directional stability coefficient, C_{L_β} = -0.0824.

Running the stability analysis for our fully loaded plane, we found our plane to be stable as well, keeping in mind that we have a lot of freedom to adjust our payload and battery if need be. The center of gravity is at 13.7", giving a static margin of 0.0476. This static margin revealed that our plane is statically stable since it is greater than zero. The analysis of the longitudinal stability coefficient showed that the contribution of the wing was stabilizing. The total longitudinal stability coefficient was a stable value of $C_{M,alpha}$ = -1.46. This is actually more stable than we would like the plane but it is still within the stable range.

The analysis of the directional stability showed that our plane is stable. Our calculations resulted in a stable coefficient of C_{n_β} = 0.0814. The lateral stability coefficient was estimated as the negative of the directional stability coefficient, C_{L_β} = -0.0814.

Final Conceptual Design

After several design decisions, the resulting conceptual design is show in the following figures.

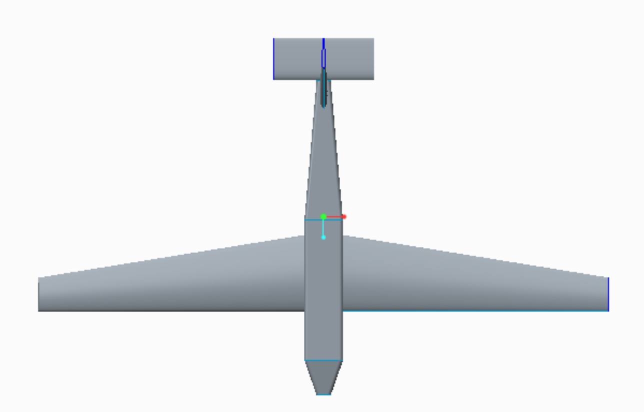

Figure 7. Top view of conceptual design.

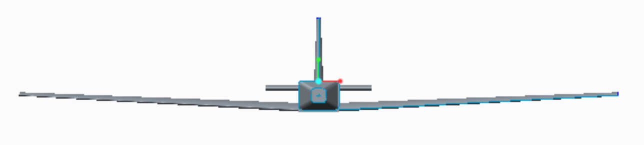

Figure 8. Front view of conceptual design

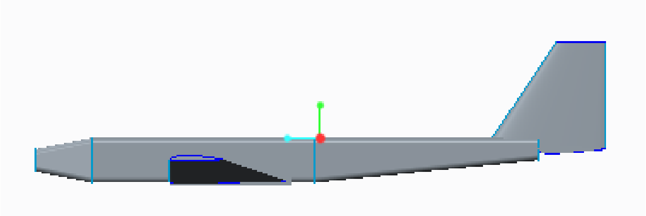

Figure 9. Side view of conceptual design.

Modifications to Conceptual Design

After presenting our conceptual design, we came away with a few modifications to our design. The main concern was that of structural strength of our fuselage which is why we planned to add triangle stock for reinforcement. This triangle stock will be added into the corners of the fuselage, especially where each section meets with another. For example, where the nosecone is bolted to the cargo bay and where the cargo bay is bolted to the tail end of the fuselage.

A major redesign to our conceptual aircraft is the redesign of our nosecone. While we originally thought of placing the moto inside the nosecone, we were informed that this design would not work. The motor needs to be able to rotate freely since, the entire motor moves when the propeller spins. With our original nosecone, this motion would be impeded and so we redesigned the nosecone to not fully encase the motor. In addition, we made the decision to add a second layer of plywood between the front of the plane's nosecone and the mount of the motor.

Detailed Design

To prepare for construction, we created detailed drawings. They are shown in Appendix B. These were the drawings used to laser cut the wood to construct our aircraft.

Modifications to Detailed Design

After reviewing our detailed drawings, we planned to make some more modifications before commencing the phase of construction. As we designed, the electronics layout was not completely clear to us and so we had to adjust our wing's ribs. We added holes to the ribs to be able to feed wire and Tygon tubing through the wing since the pitot tube would be on a wingtip and the servos for the ailerons need to be connected via wire to the flight receiver located in the cargo bay.

A second modification was to add holes to the nosecone to allow air to flow through into the fuselage. This was a suggestion made by the pilots, TA's, and professors with the main concern being the temperature of the motor and battery during flight.

Construction

Our design implemented several unique construction methods as well as some tried and true. The most common feature among all the groups was the use of a puzzle piece design. This design used interlocking groves along the edges of each piece in order to maximize joint strength and ease of construction. The only drawback to this method is that each joint needed to be nearly perpendicular. This necessitated a boxlike fuselage instead of an ovular design. Under the flight regime we were in, there was very little difference in drag between the box and ovular designs so this drawback was negligible.

One of the methods unique to our group was how we attached our wing to the fuselage. Most groups used rubber bands to keep the wing attached, however, we wanted a more robust and less wasteful design. We decided to use a series of bolts coupled with 'fish eye' grooves to accomplish this. The 'fish eye' grove looks similar to the shape of a light bulb in that one end has a circle the same radius as the head of the bolt, while the other end is a smaller circle with the same radius as the screw portion of the bolt. This allows the bolts on the fuselage to slide into the wingbox 'fish eyes' at their large ends and then slide over to the small ends. Once on the small end, the bolt stays snug. To prevent sliding in flight, two dowels were slid into separate holes going through both the fuselage and wingbox. This design proved to be very robust and created a much sturdier joint between the wing and fuselage.

In constructing our wing's main spar, we had originally planned on tapering the spar to account for the decreasing size of the ribs, but achieving the perfect taper using only the shop belt sander was a logistical nightmare. Instead, we decided to use a stair step design on the spar which had the same effect as the tapering but was much easier to construct. This method actually worked much better than the taper would have because we had the added benefit of dictating precisely where each rib would be located.

Because we had a low mounted wing, our design required the use of dihedral. Instead of building the dihedral into the wings themselves, we decided to use our wingbox as an artificial dihedral producer. This allowed us the ease of constructing a straight wing. To get dihedral from the wingbox, we used two vertical supports built in for each side of the wing. These vertical supports had holes cut out that would house the main spar and dowels in the wing, however, these holes were cut such that the holes on the inner support were slightly lower than the outer ones. This required the spar and dowels to be at the precise angle we desired for our dihedral. To create a flush connection with the root rib, the outer vertical support was angled slightly so that the front and back of the wingbox were actually trapezoidal in shape instead of rectangular.

Another unique design we implemented was the use of magnets to secure the roof of our cargo bay. The magnets held extremely well and made opening and closing the hatch simpler than other designs using rubber bands or latches. The only issue we ran into was the magnets being so strong that they would pull free from the structure because the CA wasn't strong enough. We ended up using a bit of epoxy to solidify those connections and didn't have any further issues.

Throughout the construction phase, we added triangle stock in several places along the fuselage to strengthen joints and provide more bending support. It was difficult to model this in our detailed design before we had all the electronics and passengers in their final configurations. As such, this process was more unpredictable and random than intentional but the extra support worked very well and didn't add much to the overall weight.

On the issue of weight, the construction phase proved to throw us for a loop when compared with our detailed design predictions. This discrepancy was mostly from misjudging how much glue would be used in the total construction process as well as having density values for ply and balsa being roughly the same. In actuality, the density of the ply was much larger than that of the balsa and our CAD predictions of the structure weight were vastly shy of the actual weight. A more accurate density value should be requested of the supplier to get a more accurate initial prediction.

The last unique construction design was our tail and landing gear. Early on, we made the decision to build a tail that had an airfoil instead of a flat plate. This actually turned out to be vastly easier than stick building a flat plate and performed better. There's really no reason a flat plate design should have been chosen over the airfoil design. Our vertical tail had three dowels that protruded through the root rib and slid into corresponding holes in the top of the fuselage. CA was then used to secure the connection between the rib and the fuselage. The vertical tail was actually several inches forward of the end of the fuselage so that the front of the rudder lined up with the end. This allowed the horizontal tail to be attached directly to the back of the fuselage which kept the rudder and elevator from interfering. The connection between the horizontal tail and the fuselage used two dowels lined up vertically in the center as well as two plates CA'd to the outside of the fuselage. A third dowel went through the side of the fuselage and through both plates to secure the tail from rotating on a horizontal axis. This connection worked very well in flight even though it didn't quite stand up to impact stresses.

Our tail wheel design was originally unique before all the other groups scrapped their tail wheel kits and copied us. We used a simple metal rod that went into the rudder at a 45 degree angle and then came down vertically. We had to bend the rod around the two vertical dowels in the horizontal tail wheel to allow for proper rotation and clearance. The end of the rod was bent at a 90 degree angle and the tail wheel was attached. This design was a bit structurally questionable in the beginning. The rod rotated within the rudder and this bent the whole structure sideways. A rubber band (despite our disgust with this lame form of securing stuff) was jerry rigged to the rod to keep it in place, but eventually (thank goodness!) we added a second rod further back in the rudder that then bent at a 90 degree angle and reattached to the main rod. This prevented the structure from rotating and was much more stable. A few extra rods were also soldered to the main rod to make this whole structure nigh indestructible (until we dive bombed straight into the corn field), and then it bent a little.

Performance Predictions

The table below shows the predictions for our performance metrics before any flight testing was done. These calculations were done using equations and spreadsheets taken from Thomas Corke's textbook, *Design of Aircraft*.

Table 6. Predicted performance metrics.

Metric	Units	Empty		Loaded	
		Predicted	Measured	Predicted	Measured
Weight, fuselage	lb	1.2	2		
Weight, wing	lb	1.6	3		
Weight, empty	lb	2.8	5.9		
Weight, payload				2.05	
Weight, loaded	lb			4.85	7.95
Location, CG	in.	13.5	14.05	13.8	13.95
Location, center of lift	in.	14.2	14	14.2	14
Static Margin		0.08		0.05	
Wing area	ft^2	4			
Wing span	ft	6.3			
Aspect ratio		10			
Wing loading	lb/ft^2	0.7	1.475	1.21	1.9875
Minimum level speed	ft/s	60		60	
Maximum level speed	ft/s	68		68	
Maximum rate of climb	ft/s	54.3		8.8	
Best gliding descent rate	ft/s	1.58		2.08	
Best glide speed	ft/s	18		16	
Maximum L/D		13.5		7.8	
Load factor		3		3	
Max instantaneous turn rate	deg/s	204		116	
Max sustained turn rate	deg/s	76		75	
Take-off distance	ft	80		114	
Landing distance	ft	485		545	
Lap time	s	22		24	

Flight Tests

Crash 1

The aircraft performed to our expectations during its inaugural flight in terms of maneuverability and flight-speed. It sustained damage on landing as a result of a high approach speed that caused the plane to pitch up and resume flying after briefly touching down on the forward wheels. The aircraft quickly lost lift upon leaving ground effect and rolled left, cartwheeling forward on the left wing before crashing nose first. The left wing tip was first to touch the ground; it sustained no apparent damage except for the pitot-tube which was bent ninety degrees. The nose hit the ground second and the fuselage sheared at the cargo bay section between the main wing leading edge and the nosecone, fracturing through the plywood. The horizontal stabilizer broke off at a structural weak point where it attached to the fuselage. The figure below gives an overview of the damage from the harsh landing.

The high landing speed was likely result of the aircraft's high aspect ratio (10.0) and 0.4 taper ratio, both of which lead to a decreased induced drag. Induced drag dominates other forms of drag during landing. There was also concern about a lack of elevator authority. The pilot indicated that the aircraft might have benefited from a larger elevator because it would give the aircraft more pitch control as it slowed down. A further concern was the seemingly high angle of attack on landing which might have contributed to the excess lift.

Figure 10. Photographic evidence of the damage our plane sustained from the harsh landing.

Reconstruction

Following the crash on our maiden flight, a few changes were made to the plane design as recommended by the pilots and professors. Analysis of the crash led to the discovery of its causes. First off, it was believed that on approach for landing, the plane was not able to flare sufficiently to bleed off excess speed. Therefore, the first change that was made was to increase the size of the elevator by increasing its width by a factor of 1.5 to ensure adequate pitch control on landing. In a similar vein, it was found that the plane was at too high of an angle of attack once it was fully on the ground, resulting in too much lift and a "bouncing" effect. To negate this, the rear landing gear was lengthened by 2 inches to decrease the angle of attack from 11^{o} to 7^{o}. A third change that was made was the addition of extra triangle stock in the fuselage. The structural failure after the initial crash was to be expected due to the extreme loading that the fuselage was subject to. Nevertheless, it was decided that extra support would only benefit the plane's strength and would not add substantial weight. The final change that was made came from multiple failed attempts at landing. On each of our three initial flights, the nylon bolts securing the forward landing gear ripped through the ¼" plywood in the bottom of the fuselage. In order to prevent this from happening again and to ensure that the only failure point would be the nylon bolts themselves (where it should be), an extra ¼" of plywood was added to the bottom of the fuselage where the landing gear was attached.

Crash 2

After making the modifications described in the previous section, the plane was flown again to attempt to complete the designated mission. Due to technological failure, there is regrettably no quantitative data with which to analyze the flight. However, we have video evidence of the flight and rough time measurements to work with. Initially, the plane flew spectacularly: taking tight turns and flying fast just as it was designed to do. Stopwatch measurements from the TAs recorded a lap time of 25 seconds, the fastest recorded by any group. However, nearing the end of the second lap of the mission, one of the wings came off and the plane nosedived into the ground resulting in substantial structural failure as depicted in Figure 11 below.

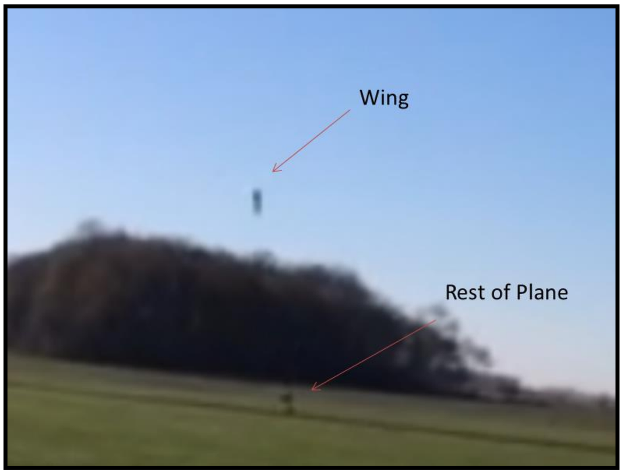

Figure 11. The problem.

Seeing the wing come off clearly explains the general idea of the plane's failure, but it is a little more difficult to understand what events took place to result in that failure. The following figures were taken directly from the video of the flight and will be explained in further detail.

Figure 12. Steady, level flight.

Figure 13. Rolling.

Figure 14. Rolled too far, upside down.

Figure 15. Nosedive.

Figure 16. Attempting to pull out of dive – wings flexing.

Figure 17. Total failure.

Figure 18. Looks of defeat.

Considering the above figures, it is easy to see the series of events that took place before the crash. The plane was initially performing well in steady, level flight. A roll maneuver was initiated that could not be corrected resulting in the airplane to begin flying upside-down. This orientation forced the nose to pitch toward the ground. In an attempt to save the plane, the pilot tried to pull the plane out of the dive. With the extremely large wingspan and flexible nature of the wing structure, the wings flexed under the high G-load and one side came off. From that point on, the flight was no longer salvageable and the crowd had to watch it meet the ground at high speed (see Ceci’s expression).

Figures 19 and 20 below show the extent of the damage at the failure point. From these, we have deduced that the glue holding the wingbox together is what failed. The first figure shows that the main spar of the wing is fully intact and seems to have simply slid out of the wingbox. The second figure shows the structural integrity of the frame of the wingbox, but its near total failure at the connections.

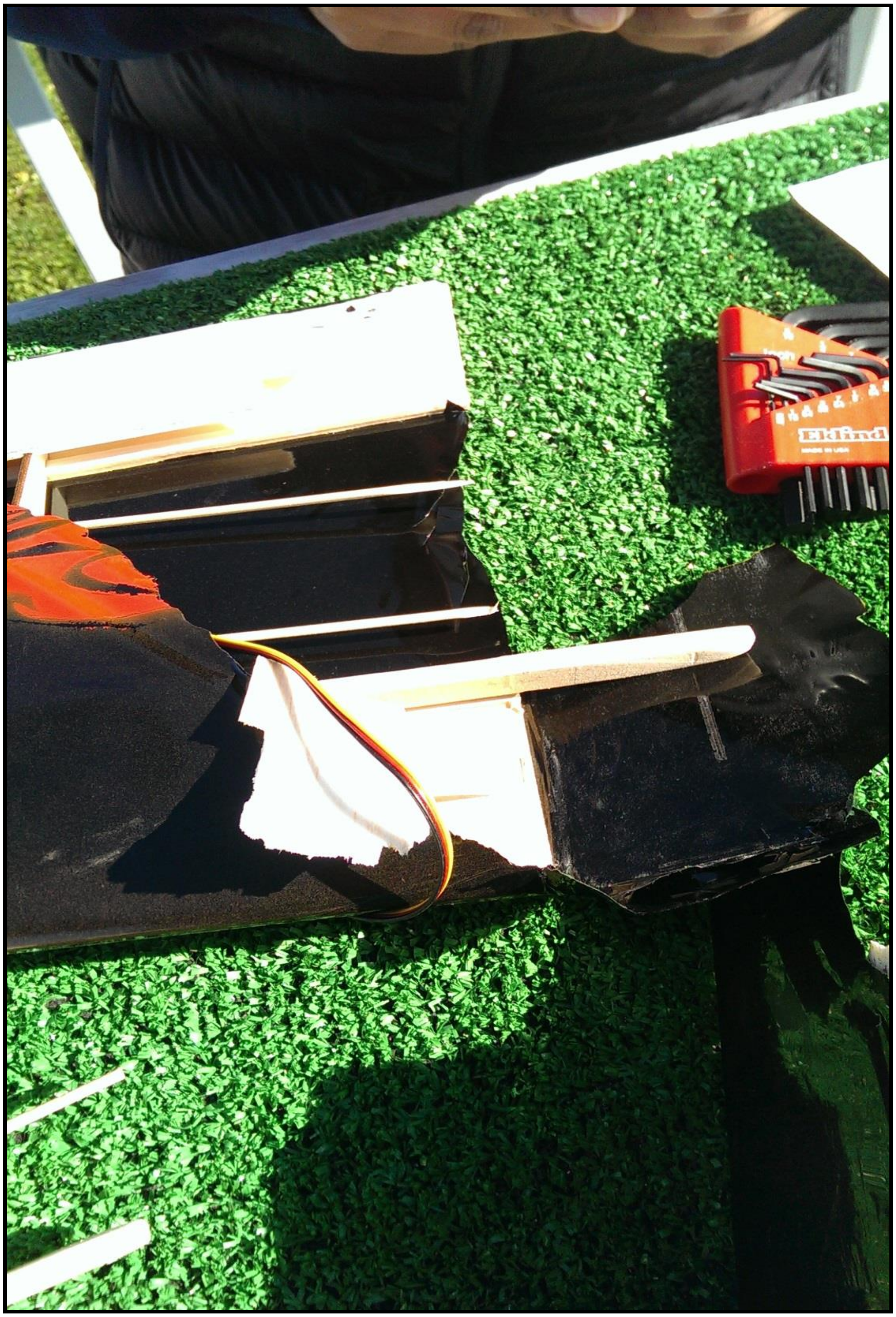

Figure 19. Wing after the crash.

Figure 20. Wingbox after the crash.

The root of the problem has yet to be discovered. What caused the initial rolling motion? The initial thought that came to mind was pilot error, the pilot simply put in too much aileron and rolled the plane. But these pilots have years of experience and the roll occurred at a point in the lap where no turning should have been done, so that possibility will be ruled out for now. The most likely scenario was that the wing was already slightly damaged from multiple rough landings and hard turns. This minor damage caused one side of the wing to stall and created the rolling moment that initiated the crash. It is difficult to determine the cause of the crash without detailed accounts from the pilot or data from the numerous electronics mounted in the plane, but this structural fatigue is the most likely cause.

Mission Analysis

Though our aircraft's final flight ended in a fatal crash, we were able to gather some insight into the completion of the mission. All of our design decisions were made with the intent of making a fast, maneuverable plane. From the one timed lap we do have, we accomplished this objective with a 25 second lap time. This is a remarkably close number to our estimated lap time of 22 seconds in an unloaded case (see Performance Prediction section above). As for our ground mission, we were able to accomplish a time of 82.6 seconds. We believe that our magnetized cargo bay was a very efficient design that allowed easy access to our cargo bay and thus helped us with our ground mission.

Unfortunately, we were not able to accomplish the entire mission but in the end, our team was content with the decisions we made when designing and constructing our plane.

Final Recommendations

We estimated our takeoff weight with a common density value for plywood that did not reflect the properties of the plywood we ultimately purchased. This proved costly as our assembled plane was almost two pounds heavier than anticipated. It would be our recommendation to over-estimate the weight of future planes to account for not only material uncertainties but also to factor in the noticeable weight contributions from glue and monokote.

We designed our control surfaces sizes to meet those indicated by conventional sizing equations. In retrospect, we could have made them considerably larger with minimal weight or structural concerns. This would have made it easier for the pilots to trim the plane to their satisfaction.

The wing, at times, felt structurally weak and displaced significantly at the tips. While it was able to sustain level flight and make controlled turns it might have benefited from a second hardwood spar. Had the plane not possessed dihedral, we could have used a single spar from wingtip to wingtip, going through the wingbox to stiffen the wing.

Finally it would have been useful to plan out the electronics layout while designing the fuselage. If we had considered the electronics arrangement more we might have allocated cargo bay space differently Further consideration would have saved some improvising towards the end of construction.

References

AME 40462: Aerospace Design II. Web. Spring 2015. < http://www3.nd.edu/~ame40462/>.

Corke, Thomas C. Design of Aircraft. Upper Saddle River, N.J.: Prentice Hall, 2003. Print.

Appendix A: Conceptual Design Spreadsheets

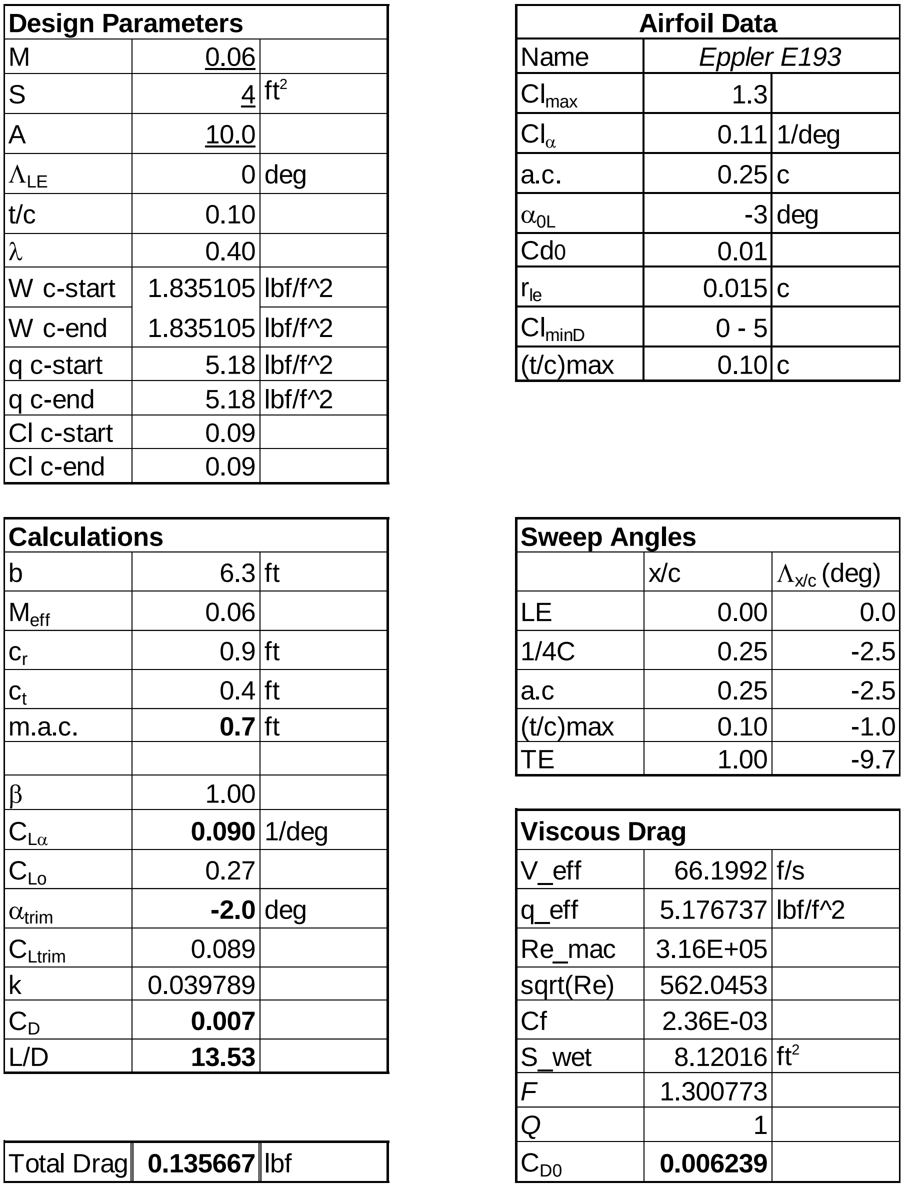

Design Parameters		
M	0.06	
S	4	ft^2
A	10.0	
Λ_{LE}	0	deg
t/c	0.10	
λ	0.40	
W c-start	1.835105	lbf/f^2
W c-end	1.835105	lbf/f^2
q c-start	5.18	lbf/f^2
q c-end	5.18	lbf/f^2
Cl c-start	0.09	
Cl c-end	0.09	

Calculations		
b	6.3	ft
M_{eff}	0.06	
c_r	0.9	ft
c_t	0.4	ft
m.a.c.	**0.7**	ft
β	1.00	
$C_{L\alpha}$	**0.090**	1/deg
C_{Lo}	0.27	
α_{trim}	**-2.0**	deg
C_{Ltrim}	0.089	
k	0.039789	
C_D	**0.007**	
L/D	**13.53**	

Total Drag	**0.135667**	lbf

Airfoil Data		
Name	*Eppler E193*	
Cl_{max}	1.3	
Cl_{α}	0.11	1/deg
a.c.	0.25	c
α_{0L}	-3	deg
Cd0	0.01	
r_{le}	0.015	c
Cl_{minD}	0 - 5	
(t/c)max	0.10	c

Sweep Angles		
	x/c	$\Lambda_{x/c}$ (deg)
LE	0.00	0.0
1/4C	0.25	-2.5
a.c	0.25	-2.5
(t/c)max	0.10	-1.0
TE	1.00	-9.7

Viscous Drag		
V_eff	66.1992	f/s
q_eff	5.176737	lbf/f^2
Re_mac	3.16E+05	
sqrt(Re)	562.0453	
Cf	2.36E-03	
S_wet	8.12016	ft^2
F	1.300773	
Q	1	
C_{D0}	**0.006239**	

Figure A - 1. Wing design calculations.

Main Wing Reference			Air Properties		
b	6.3	ft	Cruise Alt.	200	ft
m.a.c.	0.7	ft	V	66.20	f/s
S	4	ft^2	ρ	0.076074	lbm/f^3
M	0.06		q	5.176737	lbf/f^2
Λ_{LE}	0	deg	μ	1.07E-05	lbm/(f-s)
t/c	0.10		ν (cruise)	0.000141	f^2/s
λ	0.40				

Vertical Tail								
Design Parameters			**Airfoil Data**					
Cvt	*0.07*		Name	*Eppler 472*				
Lvt	*2.3*	ft	Cl_{max}	*1.3*				
Λ_{LE}	*0*	deg	Cl_{α}	*0.12*	1/deg			
t/c	*0.12*		a.c.	*0.25*	c			
λ	*1.00*		α_{0L}	*0*	deg			
Avt	*0.90*		Cd	*0.01*				
Calculations			**Sweep Angles**			**Viscous Drag**		
Svt	0.7840	ft^2		x/c	$\Lambda_{x/c}$ (deg)	V_eff	66.1992	f/s
b	0.8	ft	LE	0.00	0.0	q_eff	5.176737	lbf/f^2
c_r	0.9	ft	1/4 chord	0.25	0.0	M_eff	0.06	
c_t	0.9	ft	(t/c)max	0.35	0.0	Re_mac	439280.8	
m.a.c.	0.9	ft	TE	1.00	0.0	sqrt(Re)	662.7826	
β	1.00					Cf	2.00E-03	
$C_{L\alpha}$	**0.024**	1/deg				S_wet	1.59889	ft^2
						F	1.089468	
						Q	1.05	
Total Drag	**0.019**	lbf				C_{D0}	**0.004674**	

Horizontal Tail					
Design Parameters			**Airfoil Data**		
Cht	0.40		Name	*Eppler 472*	
Lht	2.3	ft	Cl_{max}	*1.3*	
Λ_{LE}	0	deg	Cl_{α}	*0.12*	1/deg
t/c	0.12		a.c.	*0.25*	c
λ	1.00		α_{0L}	*0*	deg
Aht	3.00		Cd	*0.01*	

Calculations			**Sweep Angles**			**Viscous Drag**		
Sht	0.4978	ft^2		x/c	$\Lambda_{x/c}$ (deg)	V_eff	66.1992	f/s
b	1.2	ft	LE	0.00	0.0	q_eff	5.176737	lbf/f^2
c_r	0.4	ft	1/4 chord	0.25	0.0	M_eff	0.06	
c_t	0.4	ft	(t/c)max	0.35	0.0	Re_mac	191717.9	
m.a.c.	0.4	ft	TE	1.00	0.0	sqrt(Re)	437.856	
β	1.00					Cf	3.03E-03	
$C_{L\alpha}$	**0.059**	1/deg				S_wet	1.015168	ft^2
						F	1.089468	
						Q	1.05	
Total Drag	**0.018**	lbf				C_{D0}	**0.007076**	

Figure A - 2. Tail design calculations.

Center of Gravity		
X_cg / L	0.3	
X_cg (ft)	1.125	f
Static Margin		
S.M.	0.07142857	stable

Longitudinal Stability Coefficient:		
Wing Parameters:		
S_w	4	f^2
(C_L_α)_w	0.09	(deg)^-1
x_w	-0.05	f
cbar	0.7	f
Horiz. Tail Paramters:		
(C_L_α)_ht	0.059	(deg)^-1
de/dα	0	Fig. 11.3
η_ht	0.7	
l_ht	2.41666667	f
S_ht	0.6	f^2
Calculations		
V_bar_hs	0.51785714	
wing effect	-0.36833001	stable
h. tail effect	1.22541348	unstable
C_M_α	**-1.5937435**	stable

Directional Stability Coefficient:			
Wing Parameters:			
A_w	10		
Λ	0	deg	
λ	0.4		
S_w	4	f^2	
b	6.3	f	
z_w	-0.125	f	
C_L (cruise)	0.27		
Fuselage Parameters:			
h	0.33333333	f	
w	0.45833333	f	
Vol_f	0.04787095	f^3	
Vertical Tail Parameters:			
(C_L_α)_vs	0.02354106	(deg)^-1	
l_vs	2.16666667	f	
S_vs	0.784	f^2	
Λ_vs	0	deg	
Calculations			
V_bar_vs	0.06740741		
(1+dσ/dβ)q/q	0.96388	Eq[11.42]	
v. tail effect	0.08763533	Eq[11.40]	stable
fuse. effect	-0.00179602	Eq[11.44]	unstable
wing effect	0.00058012	Eq[11.43]	stable
C_n_β	**0.08641943**	stable	
C_*L*_β	**-0.08641943**	stable	

Figure A - 3. Calculations for stability coefficients of an empty aircraft design.

Center of Gravity		
X_cg / L	0.304444	
X_cg (ft)	1.141667	f
Static Margin		
S.M.	0.047619	stable

Longitudinal Stability Coefficient:		
Wing Parameters:		
S_w	4	f^2
(C_L_α)_w	0.09	(deg)^-1
x_w	-0.03333	f
cbar	0.7	f
Horiz. Tail Paramters:		
(C_L_α)_ht	0.059	(deg)^-1
de/dα	0	Fig. 11.3
η_ht	0.7	
l_ht	2.4	f
S_ht	0.6	f^2
Calculations		
V_bar_hs	0.514286	
wing effect	-0.24555	stable
h. tail effect	1.216962	unstable
C_M_α	**-1.46252**	stable

Directional Stability Coefficient:			
Wing Parameters:			
A_w	10		
Λ	0	deg	
λ	0.4		
S_w	4	f^2	
b	6.3	f	
z_w	-0.125	f	
C_L (cruise)	0.27		
Fuselage Parameters:			
h	0.333333	f	
w	0.458333	f	
Vol_f	0.047871	f^3	
Vertical Tail Parameters:			
(C_L_α)_vs	0.023541	(deg)^-1	
l_vs	2.15	f	
S_vs	0.784	f^2	
Λ_vs	0	deg	
Calculations			
V_bar_vs	0.066889		
(1+dσ/dβ)q/q	0.96388	Eq[11.42]	
v. tail effect	0.086961	Eq[11.40]	stable
fuse. effect	-0.0018	Eq[11.44]	unstable
wing effect	0.00058	Eq[11.43]	stable
C_n_β	**0.085745**	stable	
C_*L*_β	**-0.08575**	stable	

Figure A - 4. Calculations for stability coefficients of a fully loaded aircraft design.

Appendix B: Detailed Drawings

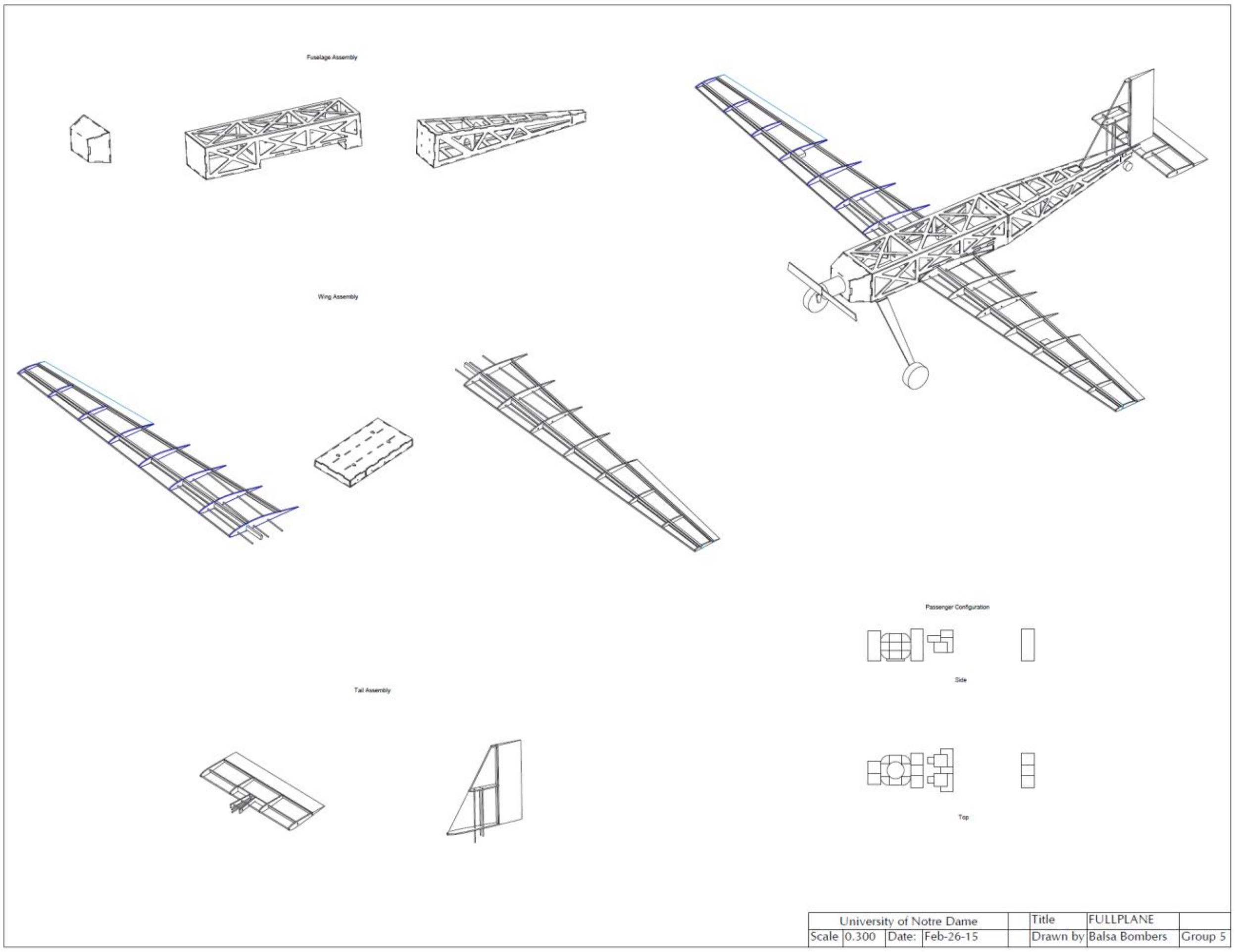

Figure B - 1. Full plane modular assembly.

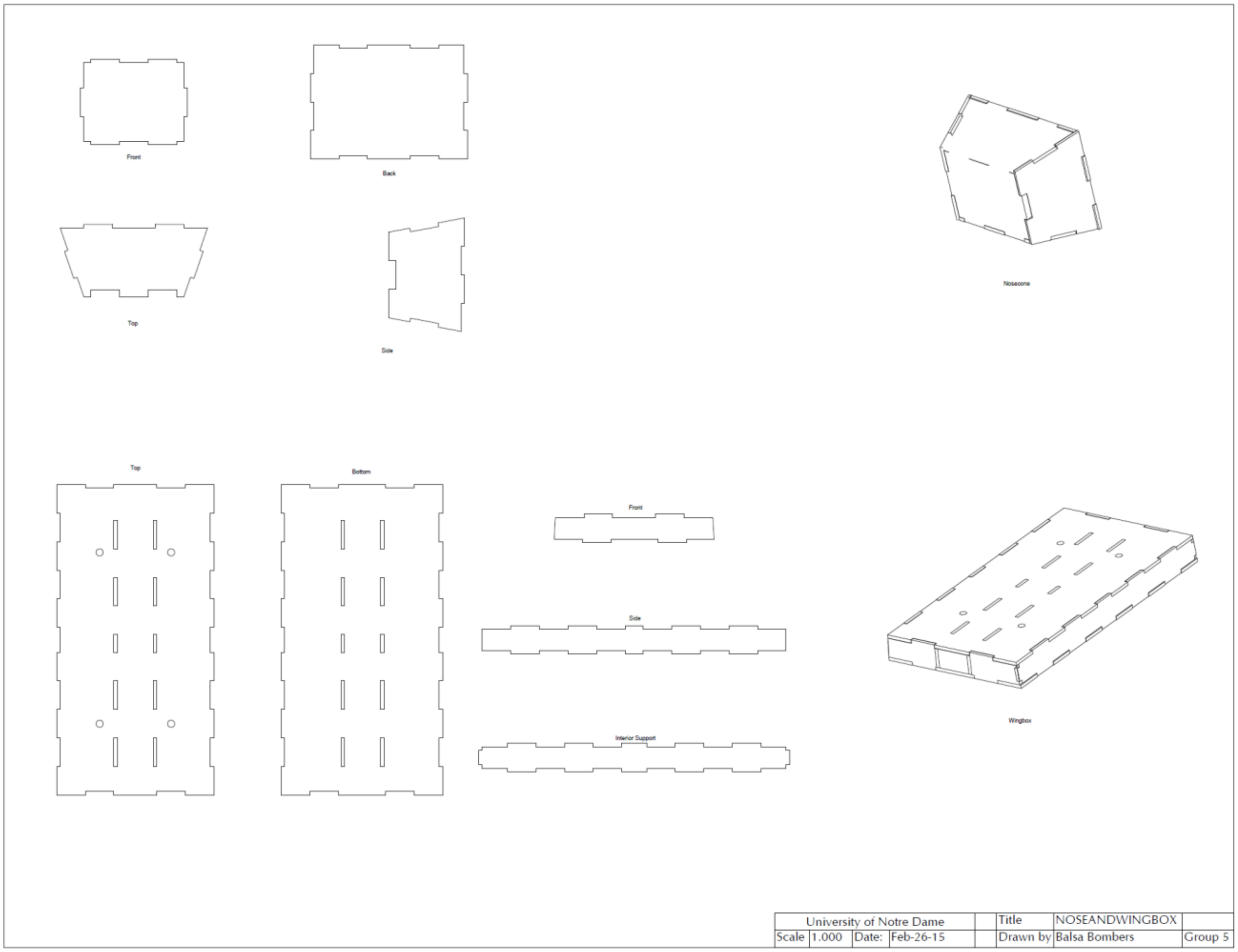

Figure B - 2. Nosecone and wingbox drawings.

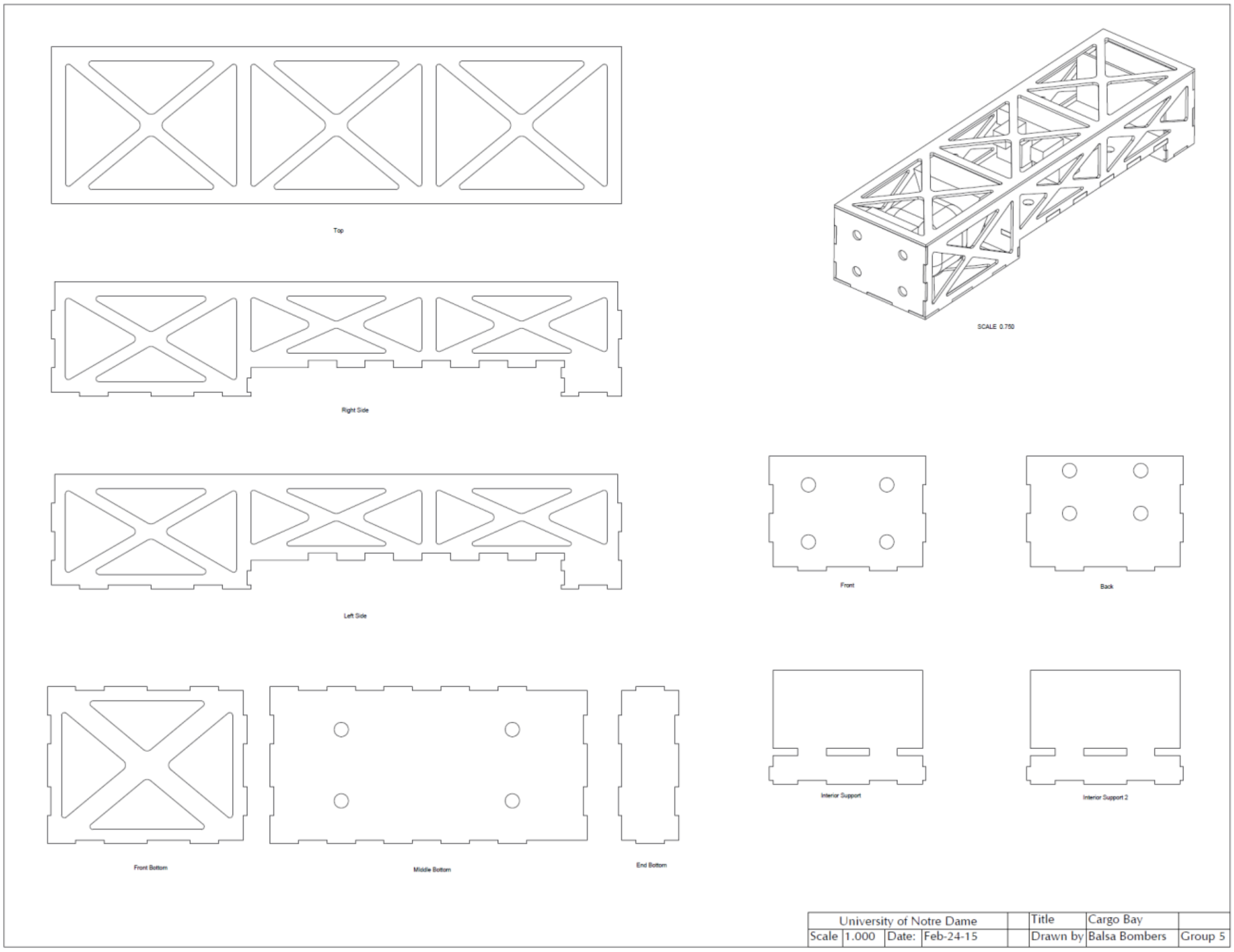

Figure B - 3. Cargo bay drawing.

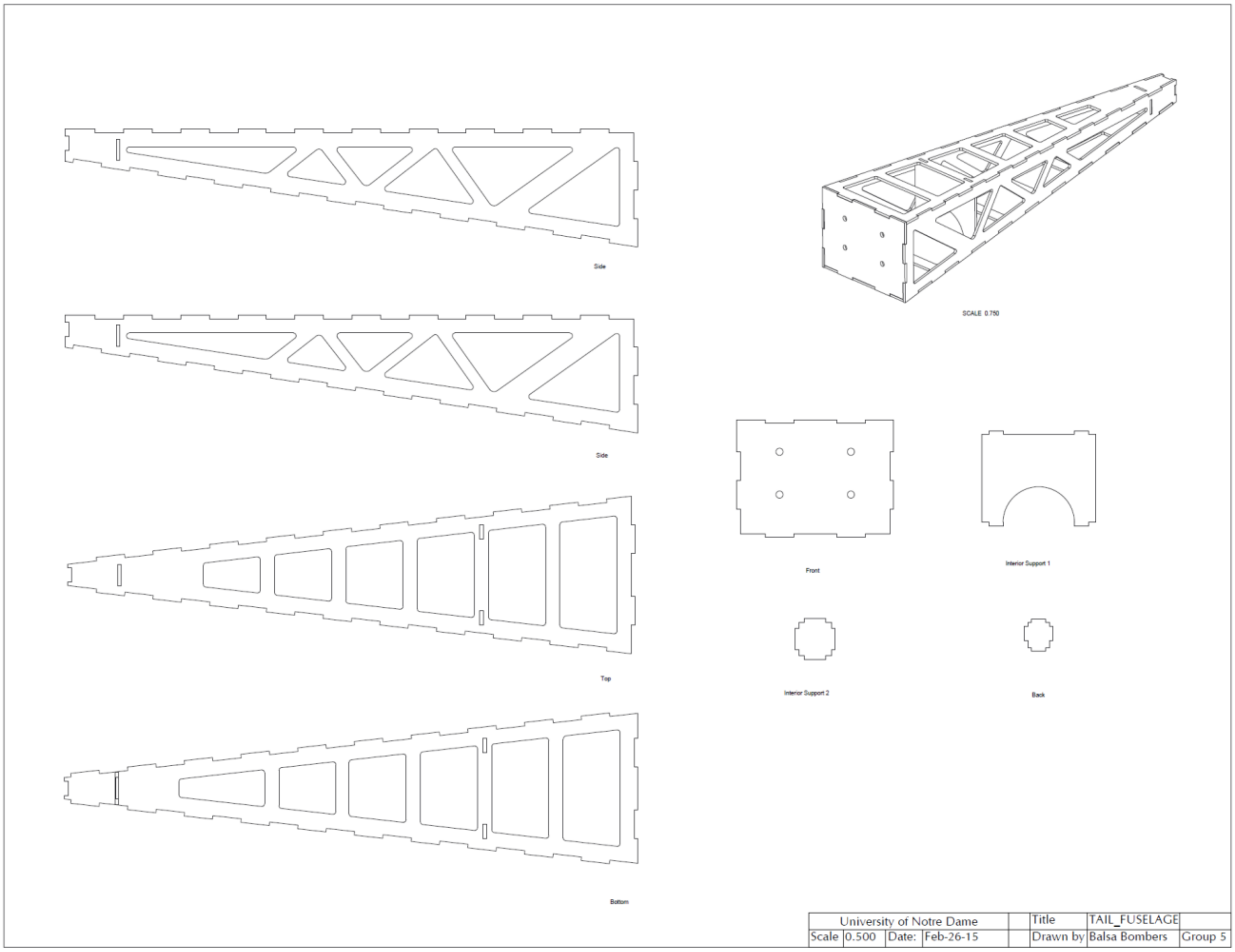

Figure B - 4. Fuselage tail drawing.

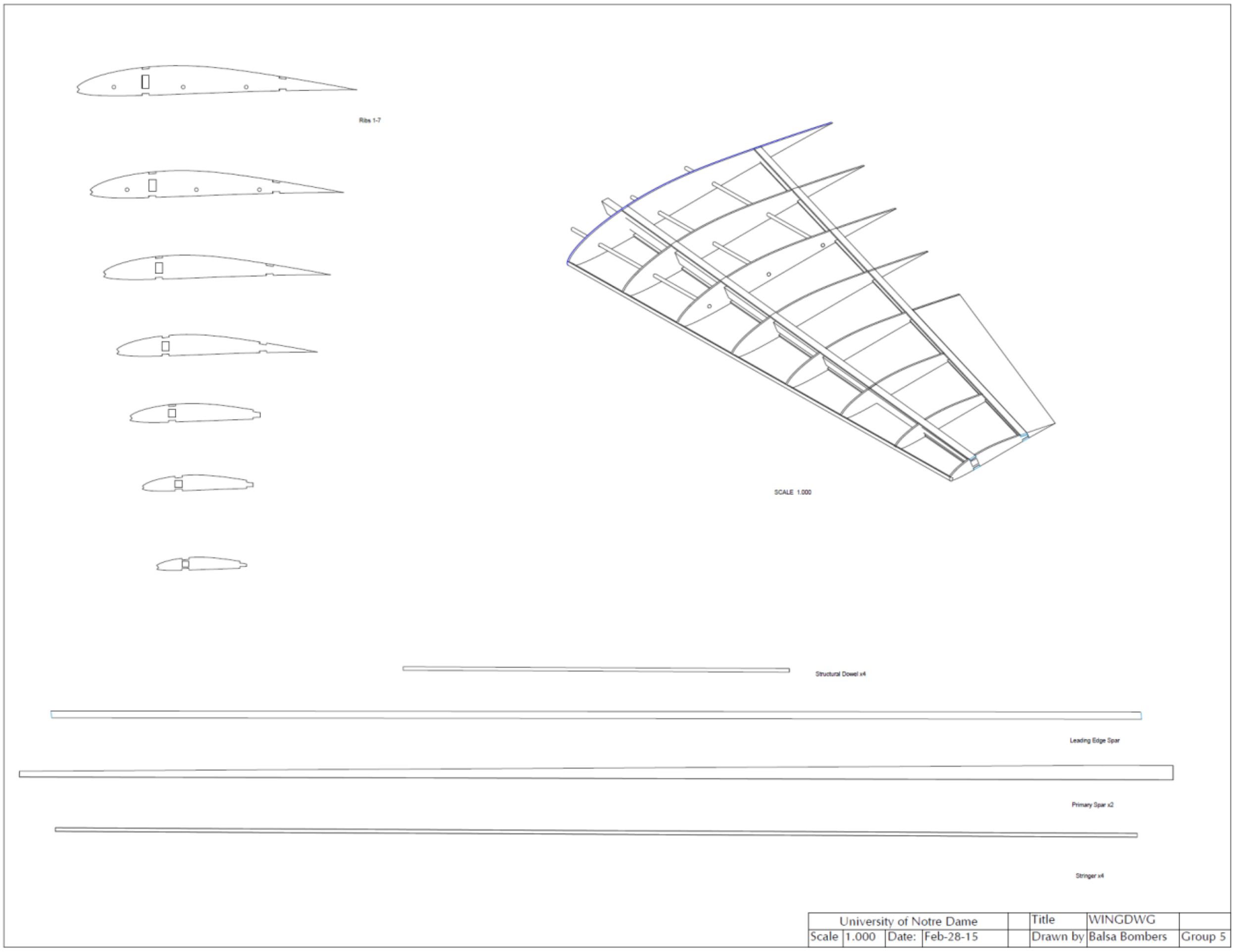

Figure B - 5. Left wing drawing.

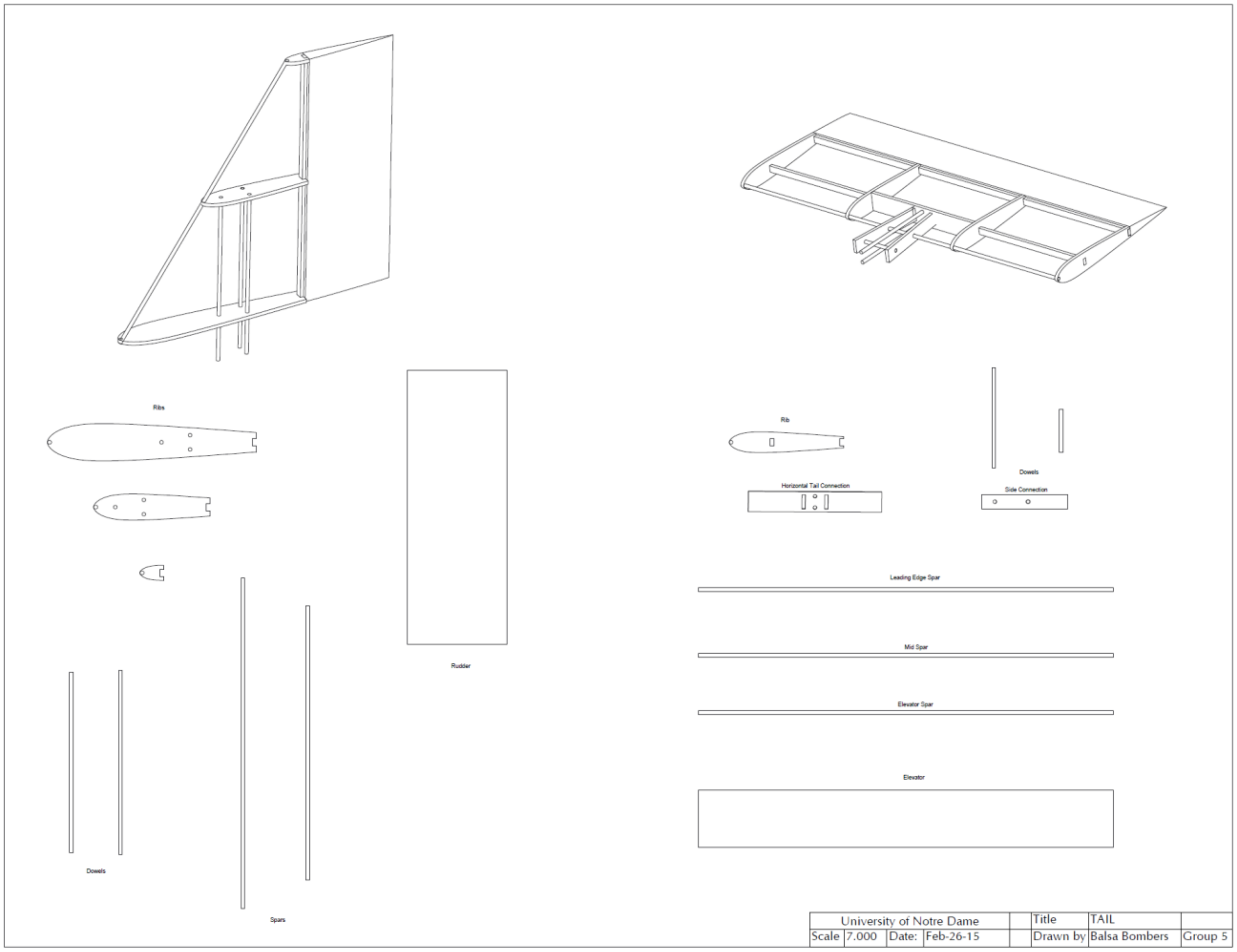

Figure B - 6. Tail drawing.

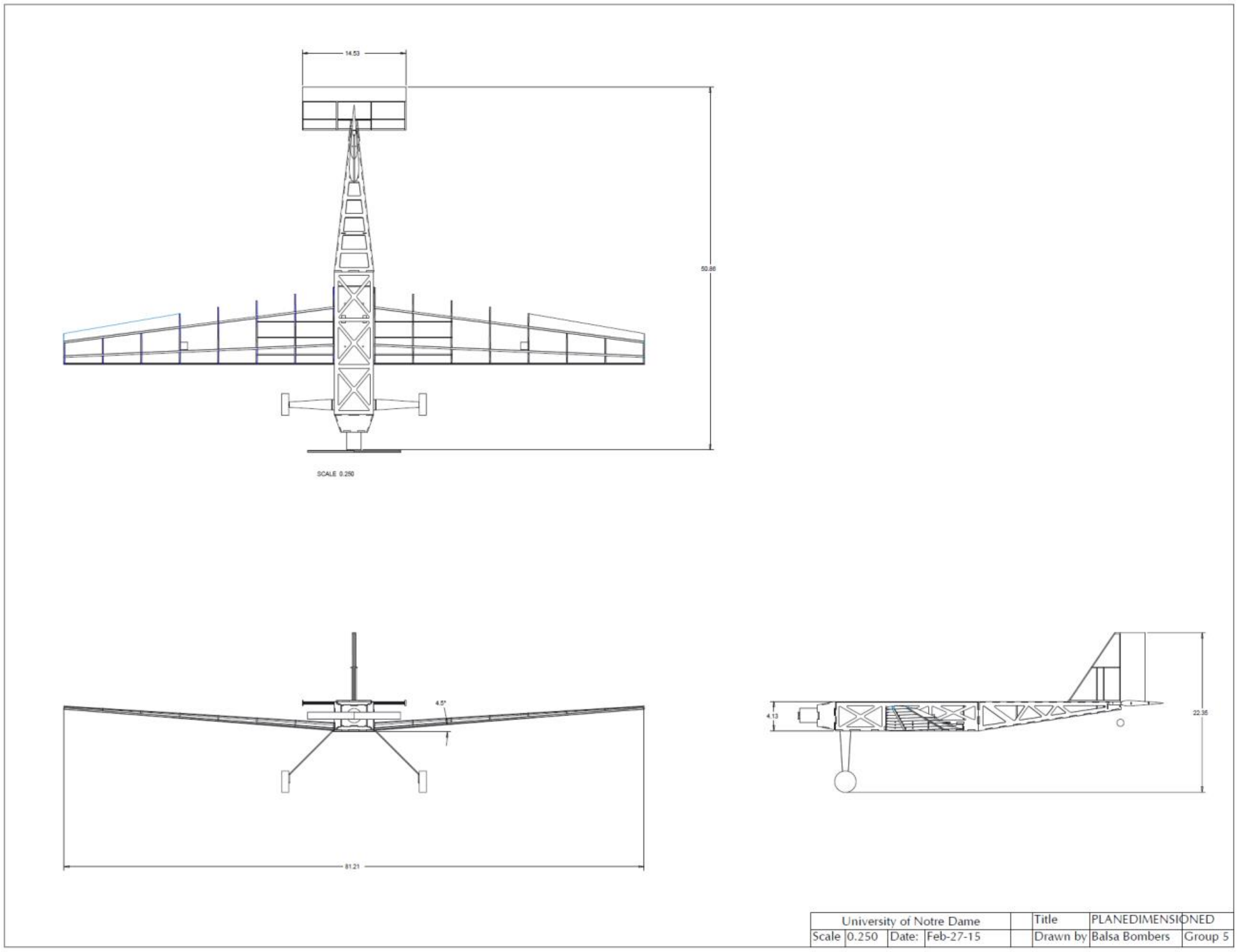

Figure B - 7. Three view aircraft drawing.

Appendix C: Video Snapshots of Fatal Crash

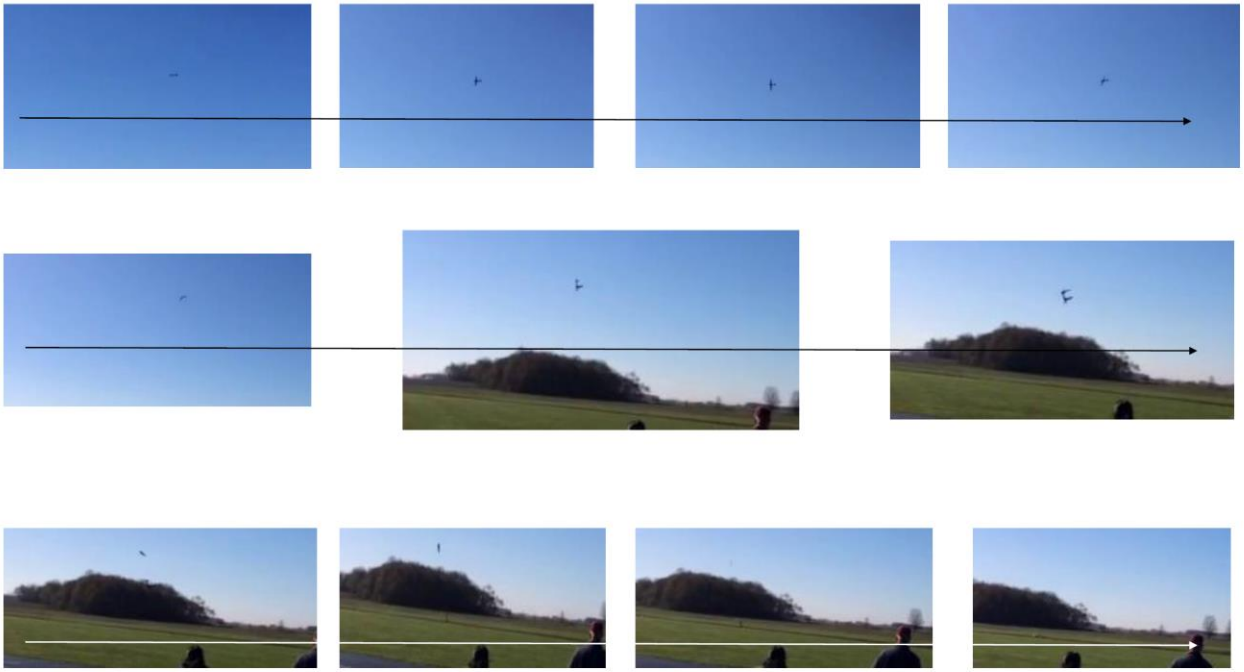

Appendix D: Senior Design Forms

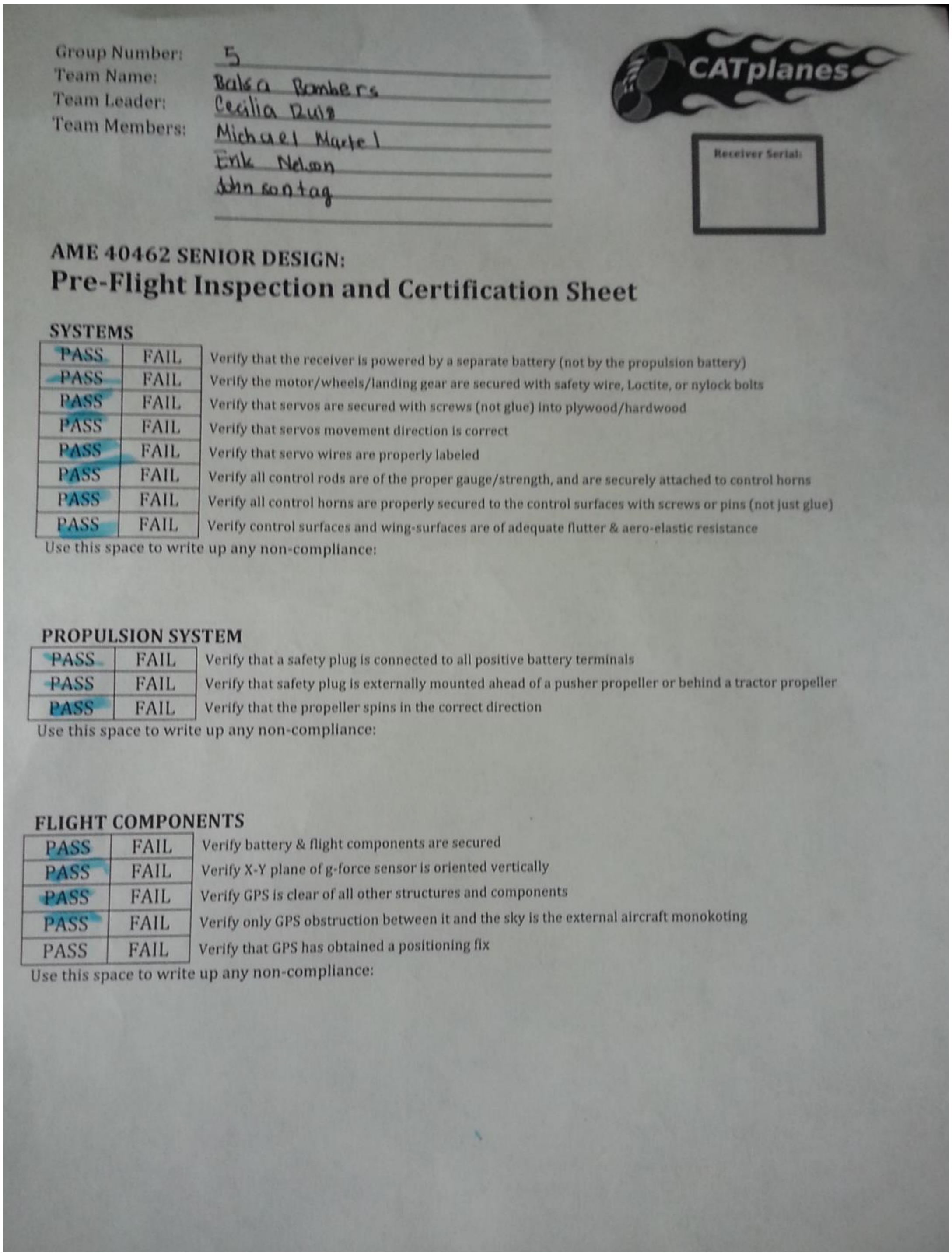

Group Number: 5
Team Name: Balsa Bombers
Team Leader: Cecilia Ruiz
Team Members: Michael Martel
Erik Nelson
John sontag

CATplanes

Receiver Serial:

AME 40462 SENIOR DESIGN:

Pre-Flight Inspection and Certification Sheet

SYSTEMS

[✓ PASS]	FAIL	Verify that the receiver is powered by a separate battery (not by the propulsion battery)
[✓ PASS]	FAIL	Verify the motor/wheels/landing gear are secured with safety wire, Loctite, or nylock bolts
[✓ PASS]	FAIL	Verify that servos are secured with screws (not glue) into plywood/hardwood
[✓ PASS]	FAIL	Verify that servos movement direction is correct
[✓ PASS]	FAIL	Verify that servo wires are properly labeled
[✓ PASS]	FAIL	Verify all control rods are of the proper gauge/strength, and are securely attached to control horns
[✓ PASS]	FAIL	Verify all control horns are properly secured to the control surfaces with screws or pins (not just glue)
[✓ PASS]	FAIL	Verify control surfaces and wing-surfaces are of adequate flutter & aero-elastic resistance

Use this space to write up any non-compliance:

PROPULSION SYSTEM

[✓ PASS]	FAIL	Verify that a safety plug is connected to all positive battery terminals
[✓ PASS]	FAIL	Verify that safety plug is externally mounted ahead of a pusher propeller or behind a tractor propeller
[✓ PASS]	FAIL	Verify that the propeller spins in the correct direction

Use this space to write up any non-compliance:

FLIGHT COMPONENTS

[✓ PASS]	FAIL	Verify battery & flight components are secured
[✓ PASS]	FAIL	Verify X-Y plane of g-force sensor is oriented vertically
[✓ PASS]	FAIL	Verify GPS is clear of all other structures and components
[✓ PASS]	FAIL	Verify only GPS obstruction between it and the sky is the external aircraft monokoting
PASS	FAIL	Verify that GPS has obtained a positioning fix

Use this space to write up any non-compliance:

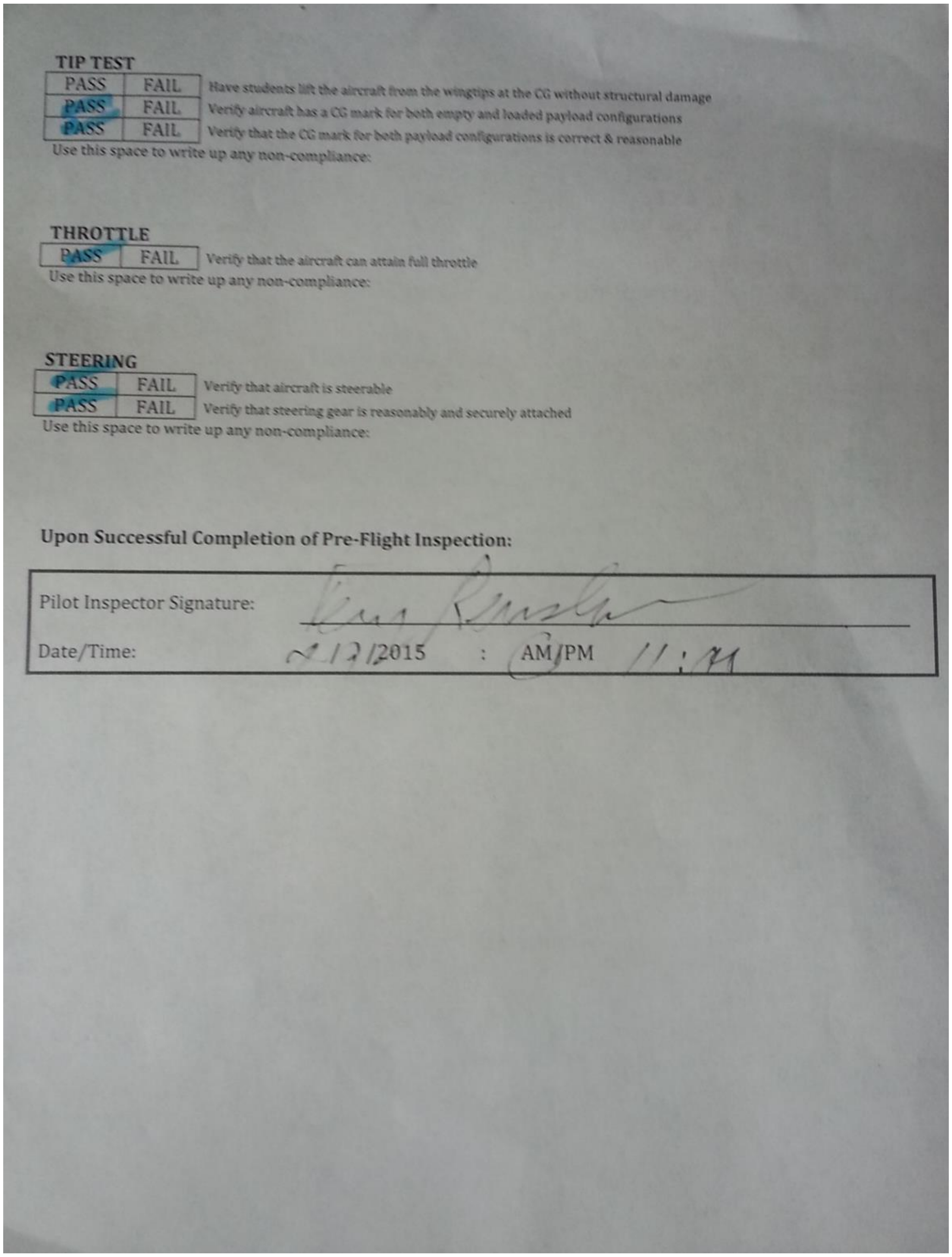

TIP TEST

PASS	FAIL	Have students lift the aircraft from the wingtips at the CG without structural damage
[✓ PASS]	FAIL	Verify aircraft has a CG mark for both empty and loaded payload configurations
[✓ PASS]	FAIL	Verify that the CG mark for both payload configurations is correct & reasonable

Use this space to write up any non-compliance:

THROTTLE

[✓ PASS]	FAIL	Verify that the aircraft can attain full throttle

Use this space to write up any non-compliance:

STEERING

[✓ PASS]	FAIL	Verify that aircraft is steerable
[✓ PASS]	FAIL	Verify that steering gear is reasonably and securely attached

Use this space to write up any non-compliance:

Upon Successful Completion of Pre-Flight Inspection:

Pilot Inspector Signature:

Date/Time: 2/12/2015 : [✓ AM]/PM 11:41

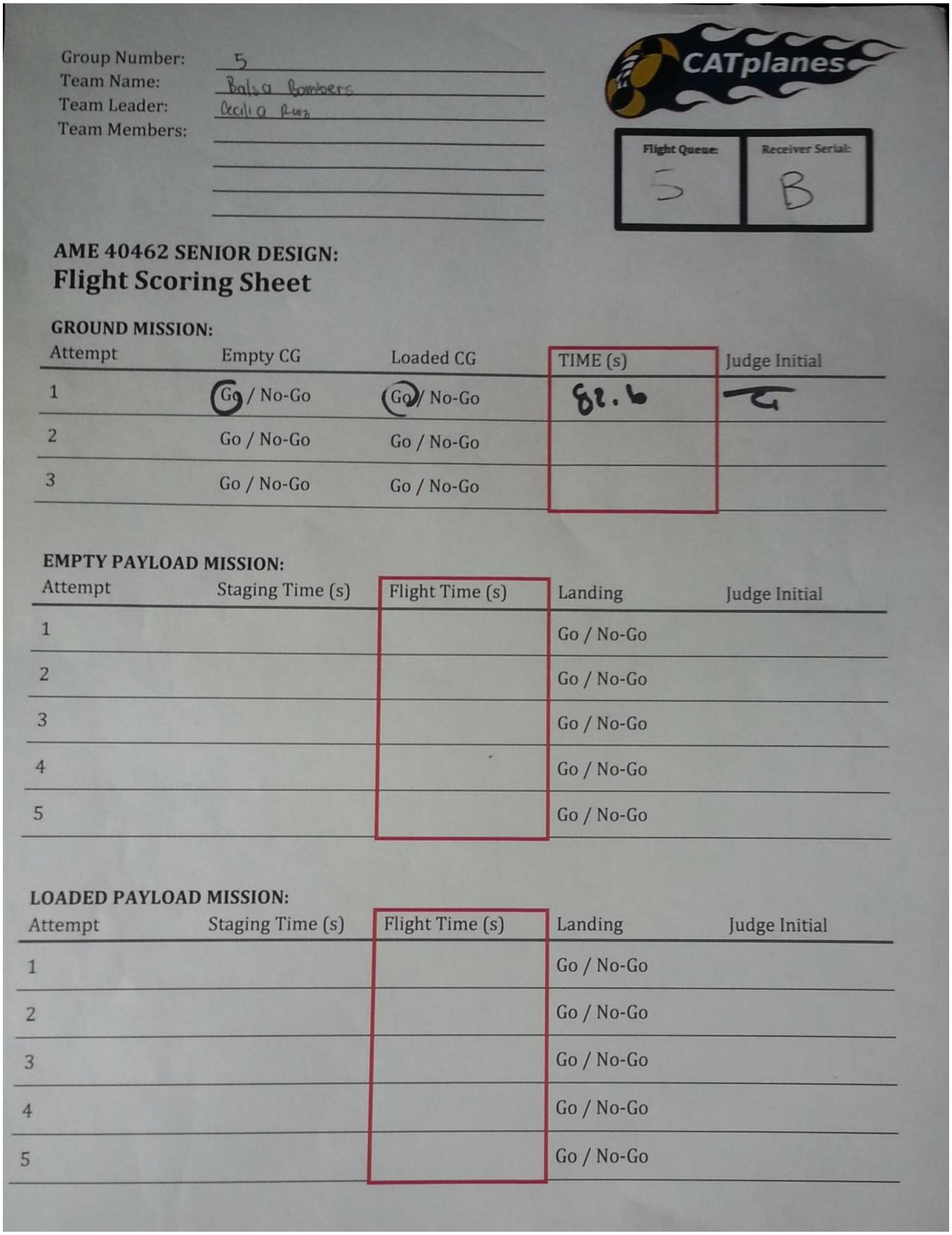

Group Number: 5
Team Name: Balsa Bombers
Team Leader: Cecilia Ruiz
Team Members:

CATplanes

Flight Queue:	Receiver Serial:
5	B

AME 40462 SENIOR DESIGN:

Flight Scoring Sheet

GROUND MISSION:

Attempt	Empty CG	Loaded CG	TIME (s)	Judge Initial
1	[✓ Go] / No-Go	[✓ Go] / No-Go	82.6	TG
2	Go / No-Go	Go / No-Go		
3	Go / No-Go	Go / No-Go		

EMPTY PAYLOAD MISSION:

Attempt	Staging Time (s)	Flight Time (s)	Landing	Judge Initial
1			Go / No-Go	
2			Go / No-Go	
3			Go / No-Go	
4			Go / No-Go	
5			Go / No-Go	

LOADED PAYLOAD MISSION:

Attempt	Staging Time (s)	Flight Time (s)	Landing	Judge Initial
1			Go / No-Go	
2			Go / No-Go	
3			Go / No-Go	
4			Go / No-Go	
5			Go / No-Go	

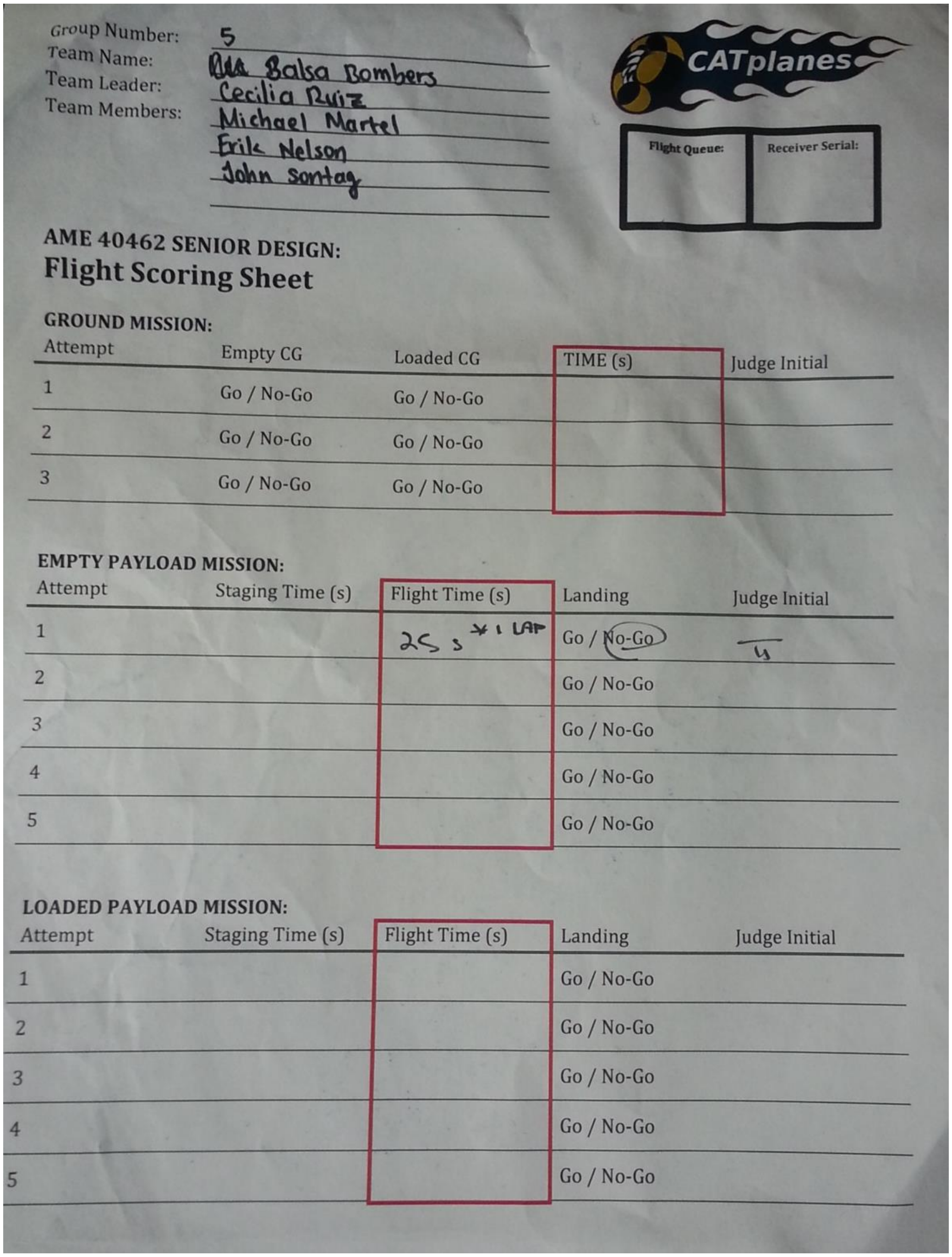

Group Number: 5
Team Name: Balsa Bombers
Team Leader: Cecilia Ruiz
Team Members: Michael Martel
Erik Nelson
John sontag

CATplanes

Flight Queue:	Receiver Serial:

AME 40462 SENIOR DESIGN:

Flight Scoring Sheet

GROUND MISSION:

Attempt	Empty CG	Loaded CG	TIME (s)	Judge Initial
1	Go / No-Go	Go / No-Go		
2	Go / No-Go	Go / No-Go		
3	Go / No-Go	Go / No-Go		

EMPTY PAYLOAD MISSION:

Attempt	Staging Time (s)	Flight Time (s)	Landing	Judge Initial
1		25 s * 1 LAP	Go / [✓ No-Go]	Ty
2			Go / No-Go	
3			Go / No-Go	
4			Go / No-Go	
5			Go / No-Go	

LOADED PAYLOAD MISSION:

Attempt	Staging Time (s)	Flight Time (s)	Landing	Judge Initial
1			Go / No-Go	
2			Go / No-Go	
3			Go / No-Go	
4			Go / No-Go	
5			Go / No-Go	